ORIGINAL RESEARCH

Dipsacus Asperoides-Derived Exosomes-Like Nanoparticles Inhibit the Progression of Osteosarcoma via Activating P38/JNK Signaling Pathway

Jiaxu Lu[1,2,*], Jiaxian Chen[2,*], Junhong Ye[2], Zhen Shi[2], Xiang Gao[1], Peicong Chen[2], Yanzhou Chang[2], Hao Lin[2], Peng Li [1]

[1]Stem Cell Research and Cellular Therapy Center, Affiliated Hospital of Guangdong Medical University, Zhanjiang, 524001, People's Republic of China; [2]Orthopedic Center, Affiliated Hospital of Guangdong Medical University, Zhanjiang, 524001, People's Republic of China

*These authors contributed equally to this work

Correspondence: Hao Lin, Orthopedic Center, Affiliated Hospital of Guangdong Medical University, Zhanjiang, 524001, People's Republic of China, Email linhao@gdmu.edu.cn; Peng Li, Stem Cell Research and Cellular Therapy Center, Affiliated Hospital of Guangdong Medical University, Zhanjiang, 524001, People's Republic of China, Email 13763086273@163.com

Introduction: Osteosarcoma is a prevalent and highly malignant primary bone tumor. However, current clinical therapeutic drugs for osteosarcoma are not suitable for long-term use due to significant side effects. Therefore, there is an urgent need to develop new drugs with fewer side effects. Dipsacus asperoides C. Y. Cheng et T. M. Ai, a traditional Chinese medicine, is commonly used for its anti-inflammatory, anti-pain, bone fracture healing, and anti-tumor effects. In this study, we investigated the effects of exosome-like nanoparticles derived from Dipsacus asperoides (DAELNs) on osteosarcoma cells in vitro and in vivo.
Methods: DAELNs were isolated and purified from Dipsacus asperoides and their physical and chemical properties were characterized using transmission electron microscopy (TEM) and nanoparticle tracking analysis (NTA). The cellular uptake of DAELNs in osteosarcoma cells was analyzed by PKH26 staining. The proliferation, invasion, migration, and apoptosis of osteosarcoma cells were assessed using CCK8 assay, EdU assay, colony-formation assay, transwell assay, wound healing assay, and mitochondrial membrane potential measurement, respectively. The regulatory mechanism of DAELNs inhibiting the progression of osteosarcoma via activating P38/JNK signaling pathway was investigated using Western blotting and immunohistochemistry. Moreover, the therapeutic effects of DAELNs were evaluated using in vivo small animal imaging assay, HE staining, and immunohistochemistry.
Results: Our results showed that DAELNs inhibited the proliferation, invasion, migration, and fostered the apoptosis of osteosarcoma cells in vitro and suppressed the tumor growth of osteosarcoma cells in a xenograft nude mouse model. Furthermore, the biodistribution of DiD-labeled DAELNs showed preferential targeting of osteosarcoma tumors and excellent biosafety in histological analysis of the liver and kidney. Mechanistically, DAELNs activated the P38/JNK signaling pathway-induced apoptosis.
Conclusion: Taken together, DAELNs are novel, natural, and osteosarcoma-targeted agents that can serve as safe and effective therapeutic approaches for the treatment of osteosarcoma.
Keywords: osteosarcoma, Dipsacus asperoides-derived exosomes-like nanoparticles, P38/JNK signaling pathway

Introduction

Osteosarcoma is the most common malignant primary bone tumor that tends to occur in adolescents, accounting for 20–34% of all primary malignant bone tumors. The current standard treatment is neoadjuvant chemotherapy-surgery-adjuvant chemotherapy based on doxorubicin, cisplatin, and high-dose methotrexate (MAP regimen).[1] Although perioperative chemotherapy has greatly improved the 5-year survival and limb salvage rates of patients with osteosarcoma, the survival benefit of brought by chemotherapy has not been further breakthroughs in the

past 40 years. 10% to 15% of patients with osteosarcoma have metastasis at the time of initial diagnosis, and the most common metastatic site is the lungs. The 5-year survival rate of patients with metastatic or recurrent osteosarcoma is only 20% and the prognosis is extremely poor. In addition, long-term toxic effects are associated with chemotherapeutics, which have limited curative efficacy.[2] Thus, it is of great significance to search for a safe and effective agent for osteosarcoma treatment.

Currently, plant exosomes, which are nanoscale vesicles secreted by plant cells and contain DNA, small RNA, microRNAs, and proteins, mediate intercellular communication.[3] Most plant exosome nanoparticles are edible and can be used as carriers to deliver specific drugs without toxicity or side effects.[4] Plant-derived exosome-like nanoparticles not only have the properties of inhibiting cancer, but can also be used as an effective anti-tumor therapy by immune regulation, tumor microcirculation remodeling, and enhancement of drug sensitivity of drug-resistant cells. It can also reduce the chemoresistance of tumor cells and alleviate the adverse reactions of other therapies through multiple signaling pathways and can be transferred to target cells to exert anti-tumor effects.[5] Plant exosomal miRNAs extracted from fresh rehmannia can reduce LPS-induced acute lung injury in mice.[6] Xia et al showed that exosomal microRNA-31, derived from halofuginone, inhibits breast cancer cell proliferation and cell cycle mediation during tumorigenesis.[7] Taken together, plant exosome nanoparticles have been found to be beneficial in multiply diseases.

Several nutritional Chinese herbs have been used to treat cancer. Dipsacus asperoides C. Y. Cheng et T. M. Ai, the roots also named XuDuan, are widely distributed in southwest China and have been used in anti-inflammatory,[8] anti-pain,[9] anti-osteoporosis,[10] bone fracture,[11] Alzheimer's disease,[12] and anti-tumor[13] treatments. Telang showed that Dipsacus asperoides inhibits proliferation and promotes apoptosis of triple-negative breast cancer cells.[14] Chen et al reported that Dipsacus asperoides polysaccharides induced apoptosis in osteosarcoma cells by modulating the PI3K/Akt pathway.[15]

Accordingly, we hypothesized that Dipsacus asperoides-derived exosome-like nanovesicles (DAELNs) would play a pivotal role in the anti-osteosarcoma activity. In this study, successfully isolated and purified DAELNs were used to explore their roles and mechanisms of action in osteosarcoma cells, both in vitro and in vivo. We found that the administration of DAELNs inhibited proliferation, migration, invasion, and apoptosis by regulating the P38/JNK signaling pathway in a dose-dependent manner. Notably, DAELNs had relatively lower toxicity and higher affinity for tumor cells in a xenograft osteosarcoma nude mouse model. Our results indicated that DAELNs could be used as promising therapeutic agents for suppressing osteosarcoma.

Methods and Materials
Isolation and Separation of the Dipsacus Asperoides-Derived Exosomes-Like Nanoparticles (DAELNs)

The dipsacus asperoides (obtained fresh from the pharmacy of Affiliated Hospital of Guangdong Medical University) were washed with running water to remove contaminants and cut into cubes. The mixture was soaked (m/v = 1:1) and incubated at 60 °C for 12 h. The obtained solution was filtered through a 70 μm sieve and centrifuged at 2500 rpm for 15 min. The supernatant was centrifuged at 10,000 × g for 30 min, filtered through a 0.45 μm filter, and the filtrate was centrifuged at 100,000 g for 70 min. The precipitate was dissolved in sterile PBS, centrifuged again at 100,000 × g for another 70 min, and the precipitate was DAELNs. After resuspension in 1 mL sterile PBS and filtration through a 0.22 μm bacterial sieve, DAELNs were quantified by a BCA assay according to the manufacturer's protocols and stored at −80 °C until further use.

Physicochemical Characterization of DAELNs

The collected DAELNs were subjected to imaging of membrane structures using transmission electron microscopy (TEM) and nanoparticle tracking analysis (NTA). Micrographs of the DAELNs were obtained using JEM-1400 series TEM (JEOL, Japan) at an accelerating voltage of 80 kV. The size and distribution of the DAELNs were determined using a NanoSight NS300 instrument (Nanosight Ltd., Navato, CA, USA) in triplicate.

Analysis of Cellular Uptake of DAELNs

To determine cellular uptake of DAELNs, HOS and MG63 cells were seeded at a density of 1×10^7 cells/mL and incubated with DAELNs at 37°C for 24 hours. The cells were then labeled with the PKH26 dye (Sigma-Aldrich, USA) according to the manufacturer's instructions. Briefly, 1 mL of Diluent C was added to the cell pellet using gentle pipetting to create a 2X cell suspension. A 2X dye solution (4 μM) was prepared by mixing 4 μL of the ethanolic PKH26 dye solution with 1 mL of Diluent C. The 2X cell suspension was rapidly added to the 2X dye solution and mixed immediately, resulting in a final concentration of 2 μM PKH26. The cultures were then incubated with DAPI (final concentration of 10 μg/mL) for 30 minutes at 37°C in the dark. Fluorescence images (both red and blue) were captured using an inverted fluorescence microscope.

Cell Counting Kit-8 (CCK-8) Assay

HOS and MG63 cells (all purchased from Procell Life Science & Technology Co., Ltd, Wuhan, China, CL0360 and CL0157) were seeded in 96-well plates (5×10^3 cells/well) and incubated with different concentrations of purified DAELNs (0, 1, 2, and 4 μg/mL) for 48 h, and 10 μL CCK8 reagent was added per well. After 1 h, the plates were then placed in a microplate reader (BioTek, USA) to detect absorbance at 450 nm.

Ethynyl-2-Deoxyuridine (EdU) Staining Assay

HOS and MG63 cells were seeded in 6-well plates (3×10^5 cells/well) and incubated with different concentrations of purified DAELNs (0, 1, 2, and 4 μg/mL) for 48 h, followed with 4% paraformaldehyde for 20 min, and treatment with 10 μM EdU at 37°C for 60 min. The cells were washed with PBS for 3 times and then permeabilized with 0.5% Triton X-100 for 15 min at room temperature, incubated with the click solution for 30 min in the dark, and then stained with Hoechst 33342 for 10 min. Fluorescence images were obtained using an inverted fluorescence microscope, and EdU-positive cells were calculated using the ImageJ software.

Colony-Formation Assay

HOS and MG63 cells were cultured in 6-well plates (1000 cells/well) in full medium for 14 days. Colonies were fixed with 4% formaldehyde for 30 min and stained with 0.1% crystal violet for 20 min. Images were taken using an inverted microscope, and colonies were counted using the ImageJ software.

Transwell Assay

Transwell chamber filters (Corning, USA) were pre-coated with 30 μL Matrigel (BD Biosciences, USA) at 37°C for 60 min in a 5% CO_2 incubator. 2×10^4 cells resuspended in 400 μL FBS-free medium were seeded into the upper chamber, and 500 μL medium supplemented with 10% FBS containing different concentrations of purified DAELNs (0, 1, 2, and 4 μg/mL) was added to the bottom chamber for 24 h. Then the non-invaded cells in the upper chamber were removed using a cotton swab, and the invaded cells were fixed with 4% formaldehyde for 30 min and stained with 0.1% crystal violet for 15 min. Images were taken using an inverted microscope, and the number of cells was calculated using the ImageJ software.

Wound Healing Assays

HOS and MG63 cells were cultured in 6-well plates (2×10^5/well) at full medium to full confluence. A wound was created by scratching the cells using a 200 μL sterile pipette tip. Floating cells were washed with PBS and cultured in full medium containing different concentrations of purified DAELNs (0, 1, 2, and 4 μg/mL) for 24 h. The wound area was photographed using an inverted microscope and measured using the ImageJ software.

Mitochondrial Membrane Potential Measurement

Changes in mitochondrial membrane potential were measured using JC-1 according to the manufacturer's instructions. HOS and MG63 cells were washed with PBS and cultured in full medium containing the JC-1

staining solution for 20 min in the dark. After washing with PBS, the cells were photographed using an inverted fluorescence microscope, and the ratio of red-to-green fluorescence intensity was measured using the ImageJ software.

Western Blotting

HOS and MG63 cells were cultured in 6-well plates and treated with different concentrations of purified DAELNs (0, 1, 2, and 4 μg/mL) for 24 h. The cells were then washed with PBS and lysed on ice with RIPA lysis buffer supplemented with protease and phosphatase inhibitors. Equal amounts protein (30 μg) were separated by 10% SDS-PAGE gels and transferred to polyvinylidene difluoride (PVDF) membranes. The Membranes were blocked with 5% skim milk at room temperature for 1 h and incubated with primary antibodies (all purchased from Cell Signaling Technology) overnight at 4°C. After washing with $1 \times$ TBST, the membranes were incubated with an HRP-labeled secondary antibody, and the protein-antibody complexes were visualized using an ECL kit in a chemiluminescence detection system and quantified using the ImageJ software.

Xenograft Experiment

All animal procedures were performed in accordance with the Institutional Animal Care and Use Committee (IACUC) of Affiliated Hospital of Guangdong Medical University and approved by IACUC of Affiliated Hospital of Guangdong Medical University (AHGDMU-LAC-B-202305-0037). All animal studies complied with the principles based on the International Guiding Principles for Biomedical Research Involving Animals. 4–6 weeks female BALB/c nude mice (SCXK2019-0010) were purchased from the Liaoning Changsheng Biotechnology Company (Liaoning, China). HOS and MG63 cells (1×10^6 in 100 μL PBS) were subcutaneously injected into nude mice. Twelve nude mice were randomly divided into two groups: PBS and purified DAELNs (5 mg/100 μL) every two days with an intraperitoneal injection five times. Tumor volume was recorded every two days, and the tumors from these mice were photographed.

Histology Analysis

Tumor tissues, mouse liver, and kidneys were split into 4-μm sections, embedded in paraffin, and subjected to xylene dewaxing, dehydration in a graded alcohol series, and antigen retrieval with 3% H_2O_2 for 10 min. After blocking with 5% bovine serum albumin (BSA) for 1 h at room temperature, the sections were incubated with primary antibodies overnight. After washing in PBST three times with shaking, the sections were incubated goat and anti-rabbit IgG for 45 min at room temperature, treated with fresh 3,3-diaminobenzidine (DAB) solution, and stained with hematoxylin. The tissues were then dehydrated with a graded alcohol series, made transparent, and observed under an Olympus microscope (Olympus, Japan). The intensity was evaluated using the Image Pro Plus software. Simultaneously, the liver and kidney were stained with H&E (G1120, Solarbio, China) according to the manufacturer's protocol.

In vivo Small Animal Imaging Assay

DAELNs were incubated with DID Far-red Plasma Membrane Fluorescent Probe (Beyotime, C1039, 10 μM) for 20 min at 37°C. After centrifugation at $100,000 \times g$ for 70 min in a microcentrifuge, the supernatant was carefully discarded and the pellet was resuspended in PBS by intraperitoneal injection into mice. The distribution of DAELNs in the liver, spleen, and kidneys of the mice was detected using an in vivo Xtreme optical multimodal imaging system (Bruker, Switzerland).

Statistical Analysis

All data are shown as the mean ± SEM and were analyzed using GraphPad Prism software (version 8.0). Two-tailed Student's t-tests or one-way ANOVA and two-way ANOVA were used to determine statistical significance, with P-values < 0.05 was considered statistically significant.

1100
DovePress

International Journal of Nanomedicine 2024:19

Results

Characterization of DAELNs

DAELNs were isolated from fresh dipsacus asperoides, and the membrane structure of DAELNs was determined using transmission electron microscopy (TEM). The average size distribution and concentration of DAELNs were determined by nanoparticle tracking analysis (NTA). As shown in Figure 1A, a round-shaped vesicular morphology with a lipid bilayer structure was observed in purified DAELNs. The concentration of DAELNs was approximately 3.5×10^9 particles/ mL, and the mean particle size ranged from 100 to 200 nm (Figure 1B). The characteristic peaks of DAELNs were also different from those of the standard in the FTIR spectrum analysis (Figure 1C). In addition, the isolated DAELNs were labeled with PKH26 and co-cultured with HOS and MG63 osteosarcoma cells and the red fluorescence in these cells indicated that the DAELNs were successfully internalized (Figure 1D). Lipidomic analysis indicated that DAELNs were enriched in diacylglycerol, ether-diacylglycerols, and ox-triacylglycerols, and metabolic analysis showed that caffeoyl quinic acid, loganin, and piscidic acid were primarily consisted in DAELNs by LC-MS/MS (BiotechPark Scientific, China) (Supplemental Figure 1). These results demonstrated that DAELNs were successfully isolated.

DAELNs Suppressed the Proliferation of Osteosarcoma Cells

To determine the effects of DAELNs on osteosarcoma cell viability, HOS and MG63 cells were incubated with different concentrations of purified DAELNs (0, 1, 2, and 4 μg/mL) for 48 h. DAELNs significantly suppressed osteosarcoma cell proliferation (Figure 2A). Both EdU staining (Figure 2B) and colony formation assays (Figure 2C) showed that the number of EdU-positive cells and colonies significantly decreased after treatment with DAELNs.
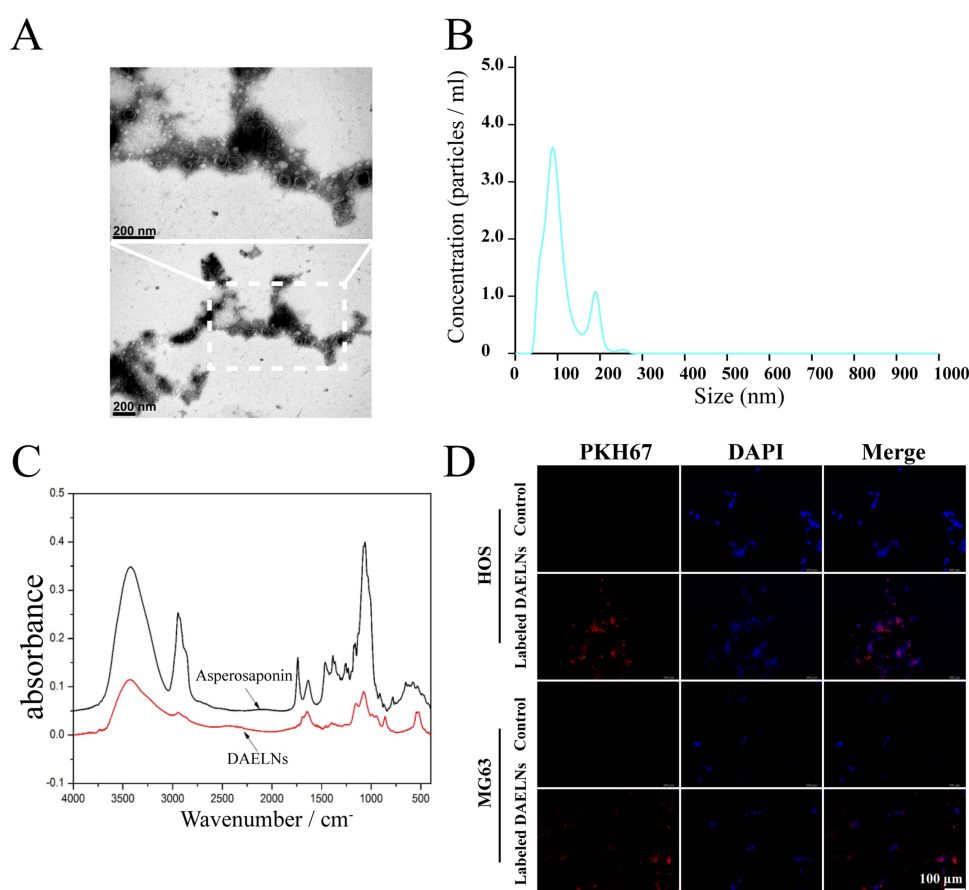

Figure 1 Characterization of DAELNs. (**A**) The membrane structure of DAELNs by transmission electron microscopy (TEM). (**B**) The average size distribution and concentration of DAELNs by nanoparticle tracking analysis (NTA). (**C**) The characteristic of DAELNs by FTIR spectrum analysis. (**D**) The internalization of DAELNs labeled with PKH26 and co-cultured with HOS and MG63 osteosarcoma cells.
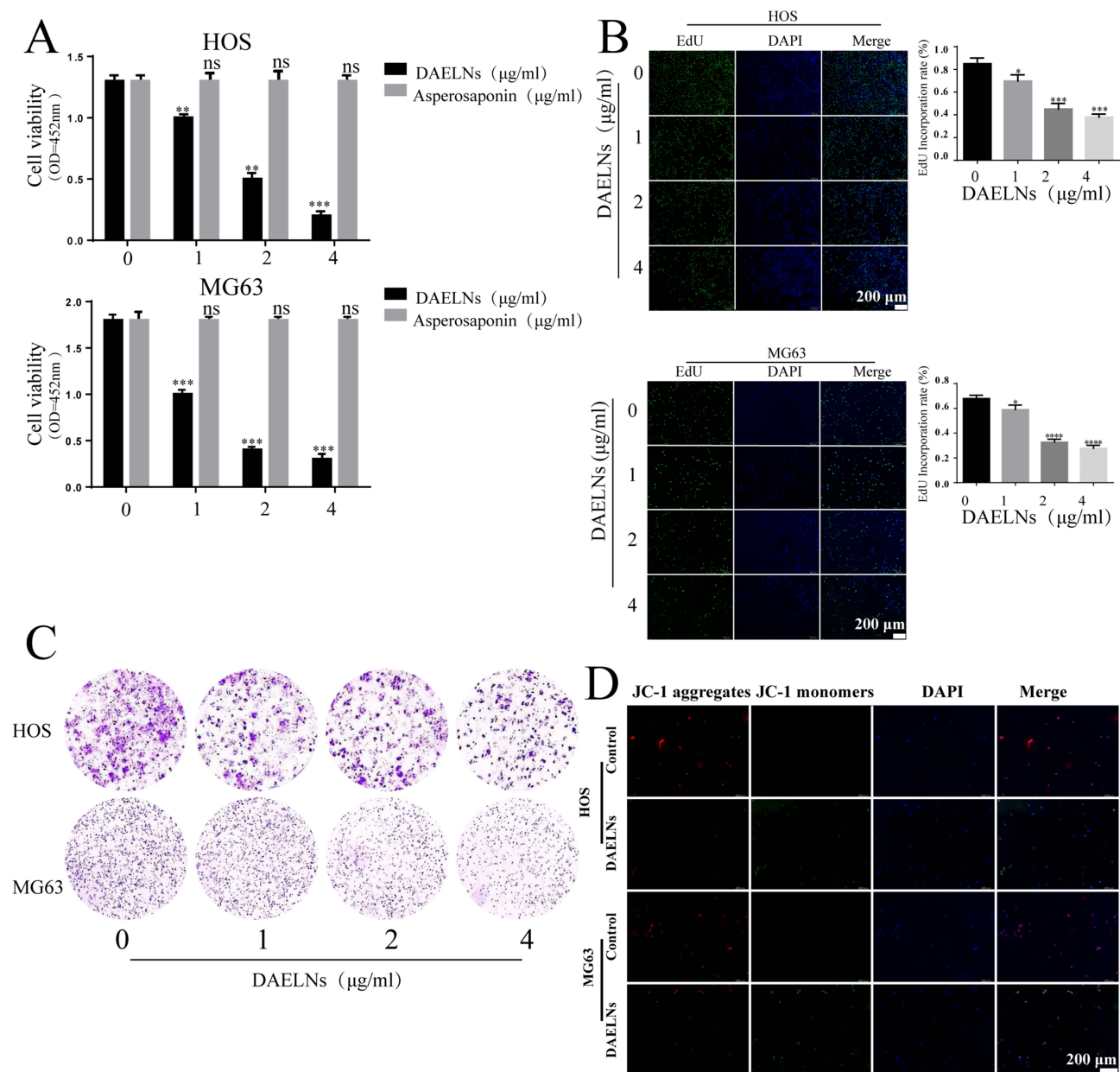
Figure 2 DAELNs suppressed the proliferation of osteosarcoma cells. (**A**) The proliferation of HOS and MG63 cells with administration of DAELNs by CCK8 assay. (**B**) The EdU staining of HOS and MG63 cells with administration of DAELNs. (**C**) The colony formation of HOS and MG63 cells with administration of DAELNs. (**D**) The mitochondrial membrane potential of HOS and MG63 cells with administration of DAELNs by JC-1 probe. Data are shown as the mean ± SEM. ns, no significance; *$P < 0.05$, **$P < 0.01$, ***$P < 0.001$ and ****$P < 0.0001$.

JC-1 dye can be used as an indicator of mitochondrial membrane potential and is widely used in apoptotic cells to monitor mitochondrial health. To determine the role of DAELNs in mitochondrial function, mitochondrial membrane potential was detected by fluorescence microscopy. We found decreased red fluorescence and increased green fluorescence in the DAELNs treatment group compared to the control group, indicating that DAELNs promoted mitochondrial-mediated apoptosis (Figure 2D). These data indicated that DAELNs can inhibit osteosarcoma cell proliferation.

DAELNs Inhibited the Migration and Invasion of Osteosarcoma Cells

We next explored whether DAELNs inhibited the invasion and migration of osteosarcoma cells using Matrigel-coated transwell and wound healing assays, respectively. As shown in Figure 3A, the number of HOS and MG63 cells that
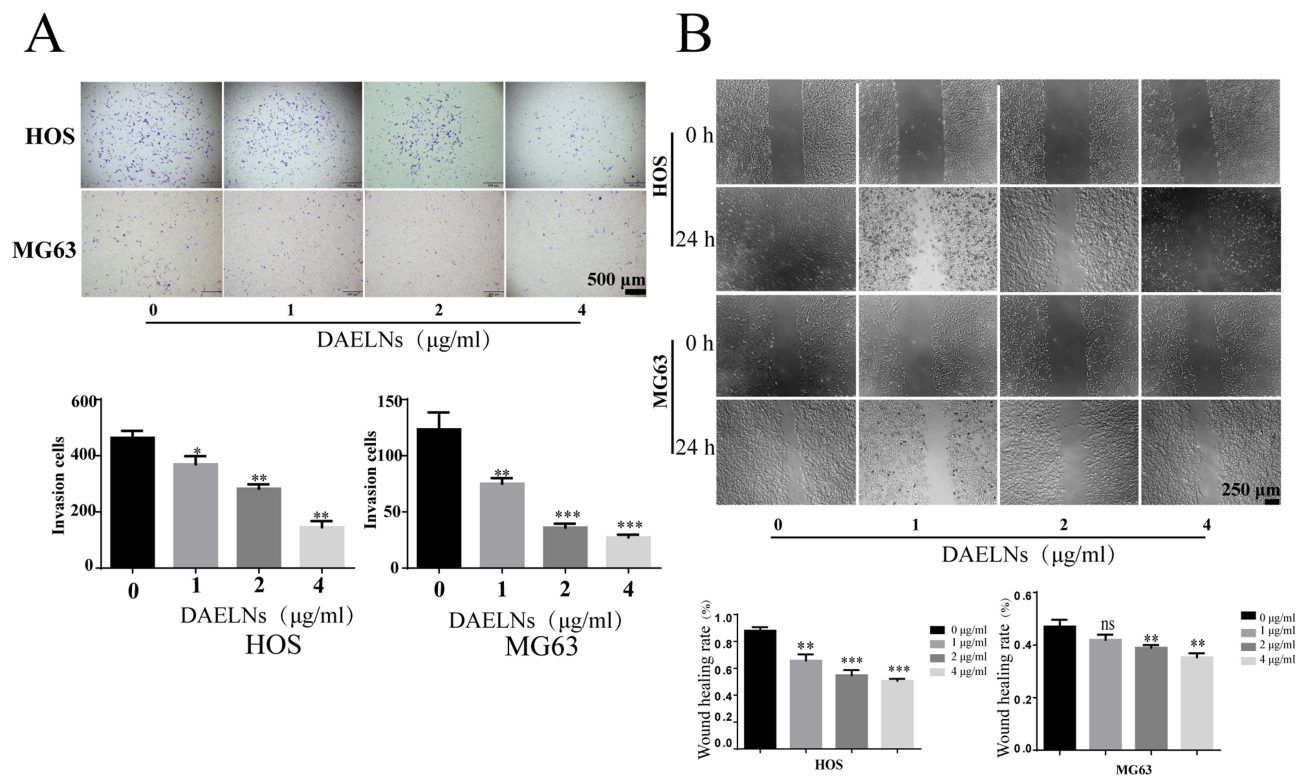
Figure 3 DAELNs inhibited the migration and invasion of osteosarcoma cells. (**A**) The invasion of HOS and MG63 cells with administration of DAELNs by Transwell assay. (**B**) The migration of HOS and MG63 cells with administration of DAELNs by wound scratch assay. Data are shown as the mean ± SEM. ns, no significance; *$P < 0.05$, **$P <$ 0.01, and ***$P < 0.001$.

passed through the membrane decreased after DAELNs treatment. In addition, the scratch healing rate of the DAELNs treatment group was significantly decreased compared with that of the control group in a dose-dependent manner (Figure 3B). These data revealed that DAELNs had a marked inhibitory effect on the invasive capability and migration of osteosarcoma cells.

Activated p38/JNK Signaling Pathway is Involved in DAELNs Induced Anti-Osteosarcoma Effects

Previous studies have demonstrated that Jun N-terminal kinase (JNK) and p38 mitogen-activated protein kinase (MAPK) signaling are associated with the proliferation, differentiation, survival, and migration of cancer cells. To further investigate the mechanism of activation of the p38/JNK signaling pathway in DAELNs treated osteosarcoma cells, we explored the protein levels of total P38, phosphorylation of P38 (P-p38), total JNK, and phosphorylation of JNK (P-JNK). We found that both P-p38 and P-JNK were increased by DAELNs treatment, indicating that DAELNs may activate p38 and JNK signaling pathways (Figure 4). Western blotting also showed that the expression of Bcl2 was impeded, and the Bax profile was boosted in the DAELNs group in a dose-dependent manner (Figure 4). These findings suggested that the anti-osteosarcoma effects of DAELNs may be related to the activation of p38/JNK signaling-induced apoptosis.

DAELNs Inhibits Tumor Growth of Osteosarcoma Cells in vivo

To evaluate the targeting ability and bio-distribution of DiD-labeled DAELNs in the osteosarcoma mouse model, the fluorescence intensity of DiD-labeled DAELNs was imaged of several organs including the osteosarcoma tumor, spleen, liver and kidney using an in vivo imaging system (IVIS) at different time points. Figure 5A shows higher fluorescence intensity in osteosarcoma tumors after a time period of 24 h, which increased over time. The fluorescence intensity
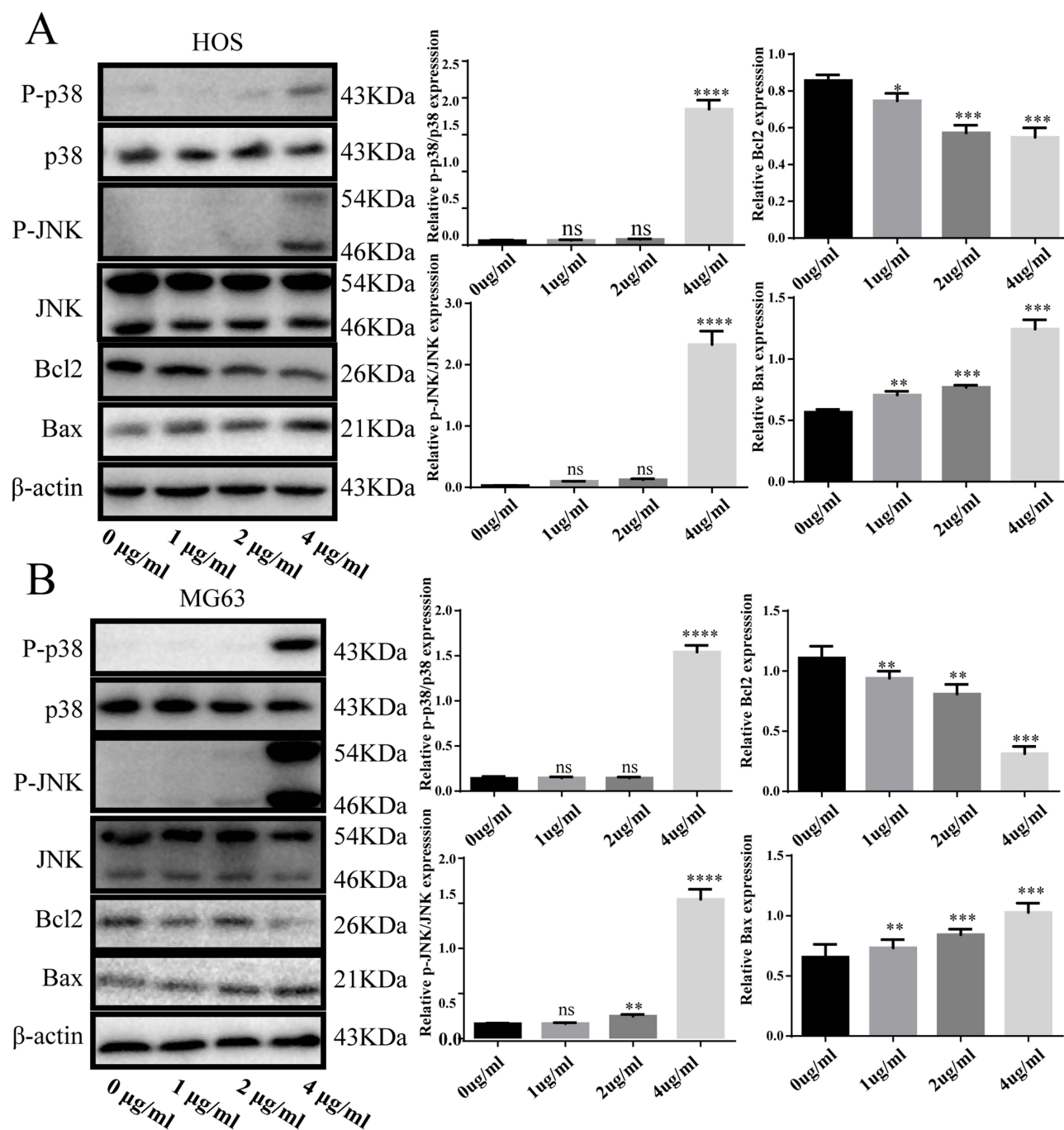
Figure 4 Activated p38/JNK signaling pathway is involved in DAELNs induced anti- osteosarcoma effects. (**A**) The expression of P-p38, P38, P-JNK, JNK, Bax and Bcl2 in HOS cells with administration of DAELNs by Western blotting. (**B**) The expression of P-p38, P38, P-JNK, JNK, Bax and Bcl2 in MG63 cells with administration of DAELNs by Western blotting. Data are shown as the mean ± SEM. ns, no significance; *$P < 0.05$, **$P < 0.01$, ***$P < 0.001$, and ****$P < 0.0001$.

decreased after 72 h in spleen, liver, and kidney tissues (Figure 5A). In addition, HE staining demonstrated that DAELNs had no side effects on the liver and kidneys (Figure 5C). These data indicate that DAELNs preferentially target of osteosarcoma tumors.

Finally, we established a xenograft mouse model to validate the anti-osteosarcoma effects of DAELNs in vivo. We found that DAELNs inhibited the growth of osteosarcoma cells compared to the control group (Figure 5B). The osteosarcoma samples were analyzed using H&E and IHC staining. No significant histological damage was observed in the control group, whereas the DAELNs treated group showed a significant reduction in the area. Moreover, we found that DAELNs inhibited the expression of
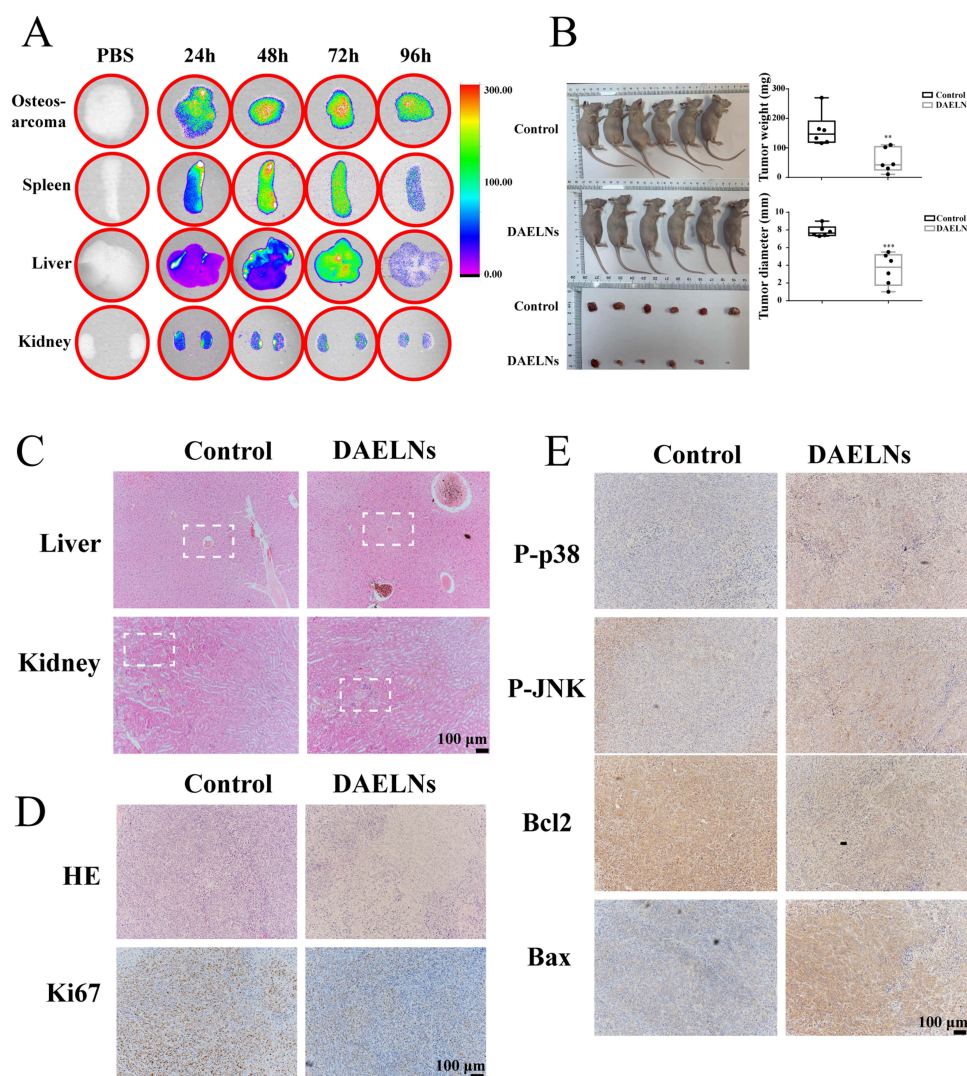
Figure 5 DAELNs inhibits tumor growth of osteosarcoma cells in vivo. (**A**) The bio-distribution of DiD-labeled DAELNs in tumor, spleen, liver and kidney tissues from the osteosarcoma mouse model by in vivo imaging system. (**B**) The tumor growth of osteosarcoma mouse model by treat with DAELNs. Data are shown as the mean ± SEM. **$P < 0.01$, and ***$P < 0.001$. (**C**) The toxicity of kidney and liver by HE staining. The white dotted square means the hepatic lobule of liver and the glomerulus of the kidney. (**D** and **E**) The H&E staining and IHC staining of tumor tissues stained with Ki67, P-p38, P-JNK, Bcl2, and Bax.

Ki67 and Bcl2 while increasing the expression of P-p38, P-JNK and Bax in osteosarcoma tissues (Figure 5D and 5E). Taken together, these data further confirm that DAELNs may inhibit the tumor growth of osteosarcoma cells in vivo via the activation of p38/JNK signaling-induced apoptosis.

Discussion

Osteosarcoma is the most common primary malignant tumor with poor prognosis in teenagers.[16] Chemotherapy is one of the common treatments for osteosarcoma.[2] The adverse effects of chemotherapy for osteosarcoma include myelosuppression, gastrointestinal reactions, liver function impairment, cardiotoxicity, renal and bladder toxicity, anaphylaxis, and skin toxicity.[17] Therefore, novel reagents with low toxicity and high efficacy are important for osteosarcoma patients. In the current study, we successfully isolated and purified exosome-like nanoparticles derived from Dipsacus asperoides, a traditional Chinese medicine, and observed antitumor effects in osteosarcoma both in vitro and in a xenograft mouse model by regulating P38/JNK signaling induced apoptosis.

Exosomes are extracellular vesicles with a diameter of 40–100 nm secreted by eukaryotic cells. Many mammalian cells can release exosomes, including reticulocytes, dendritic cells, B cells, T cells, mast cells, epithelial cells, and tumor cells.[18] Since the discovery of exosomes in animal cells, there has been growing evidence that exosome-like vesicles occur in plants. Previous

studies have shown that plant exosomes play a role in tumors, immunity, intestinal disease, inflammatory response, and drug delivery without toxicity and side effects.[4,19,20] Yun et al found that small RNAs and miRNAs from ginger-derived exosomes regulate gut microbes and their metabolites, and inhibit colitis in a mouse model.[21] Both ginger and grape exosome-like nanoparticles accelerate intestinal epithelial proliferation and promote recovery from DSS-induced colitis.[22] miRNAs in honeysuckle decoctions can be effectively absorbed, inhibiting the replication of COVID-19 and accelerating the negative conversion of infected patients.[23] In addition, miRNAs extracted from the traditional Chinese medicine Glycyrrhiza significantly inhibit T cell differentiation, inflammation, and apoptosis.[24] These studies indicate that exosomes derived from both edible plants and traditional Chinese medicines have considerable effects on human diseases.

The chemical constituents of Dipsacus asperoides mainly include triterpenoids, glycosides, iridoid glycosides, alkaloids, and volatile oil compounds. In recent years, experimental researchers have found that Dipsacus asperoides have been used as medicinal agents in anti-tumor, neuroprotection, anti-osteoporosis, bone fractures, anti-pain, anti-oxidation, anti-inflammatory, and other pharmacological effects. Chen et al also demonstrated that Dipsacus asperoides polysaccharides promote apoptosis in osteosarcoma cells by activating the PI3K/Akt pathway.[15] Here, we show that DAELNs inhibit the proliferation, migration, invasion, and accelerated apoptosis of osteosarcoma cells in a dose-dependent manner and remarkably suppress tumor growth, which provides compelling evidence of strong anti-osteosarcoma effects.

P38 is a mitogen-activated protein kinase (MAPK) involved in cell differentiation, apoptosis, and autophagy.[25] MAPKs are a family of serine/threonine kinases that comprise three major subsets, namely extracellular signal-regulated kinase (ERK), p38, and c-Jun N-terminal kinase (JNK). Cellular responses to many external stimuli involve the activation of the MAPK signaling pathway.[26] We found that DAELNs activated P38 and JNK phosphorylation in a dose-dependent manner. In addition, the expression of Bax increased, while that of Bcl2 decreased both in vitro and in tumor tissues. Moreover, the mitochondrial membrane potential by JC-1 dye staining showed that red fluorescence decreased and green fluorescence increased after DAELNs administration, indicating that DAELNs could induce mitochondrial depolarization and promote cell apoptosis.

Metabolic analysis of DAELNs also showed that caffeoyl quinic acid, loganin, and 5-methoxypsoralen primarily comprised DAELNs. Loganin has been used for its anti-inflammatory, antioxidant, and anti-tumor effects. Loganin significantly inhibits cell growth and metastasis and promotes apoptosis in gastric cancer.[23] The main metabolic products in DAELNs may also play an important role in promoting apoptosis in osteosarcoma.

At the same time, we also detect the bio-distribution of DiD-labeled DAELNs in the osteosarcoma mouse model. We found that the fluorescence intensity was always higher in tumor tissues than in spleen, liver, and kidney tissues, indicating that DAELNs preferentially target osteosarcoma tumors. Moreover, H&E staining revealed that the kidneys and liver had no side effects in the DAELN-treated mouse model. These findings validate that DAELNs may have low toxicity and high targeting ability, which may indicate that DAELNs can be considered safe and effective drugs for osteosarcoma treatment.

Conclusion

In conclusion, our study demonstrated that DAELNs can inhibit the growth of osteosarcoma in vitro and in vivo by activating the P38/JNK signaling-induced apoptotic pathways with low toxicity and high affinity, which sheds light on the effective clinical potential of plant-derived exosomes for the treatment of osteosarcoma.

Author Contributions

All authors made a significant contribution to the work reported, whether that is in the conception, study design, execution, acquisition of data, analysis and interpretation, or in all these areas; took part in drafting, revising or critically reviewing the article; gave final approval of the version to be published; have agreed on the journal to which the article has been submitted; and agree to be accountable for all aspects of the work.

Funding

Disclosure

The authors declare no conflicts of interest in this work.

References

1. Ritter J, Bielack S. Osteosarcoma. *Ann Oncol*. 2010;21:vii320–vii325. doi:10.1093/annonc/mdq276

2. Kager L, Tamamyan G, Bielack S. Novel insights and therapeutic interventions for pediatric osteosarcoma. *Future Oncol*. 2017;13(4):357–368. doi:10.2217/fon-2016-0261

3. Kalluri R, LeBleu VS. The biology, function, and biomedical applications of exosomes. *Science*. 2020;368(6489):367. doi:10.1126/science.abb5060

4. Dad HA, Gu TW, Zhu AQ, Huang LQ, Peng LH. Plant exosome-like nanovesicles: emerging therapeutics and drug delivery nanoplatforms. *Mol Ther*. 2021;29(1):13–31. doi:10.1016/j.ymthe.2020.11.030

5. Hoshino A, Kim HS, Bojmar L, et al. Extracellular vesicle and particle biomarkers define multiple human cancers. *Cell*. 2020;182(4):1044–1061 e1018. doi:10.1016/j.cell.2020.07.009

6. Qiu FS, Wang JF, Guo MY, et al. Rgl-exomiR-7972, a novel plant exosomal microRNA derived from fresh Rehmanniae Radix, ameliorated lipopolysaccharide-induced acute lung injury and gut dysbiosis. *Biomed Pharmacother*. 2023;165:115007. doi:10.1016/j.biopha.2023.115007

7. Xia X, Wang X, Zhang S, et al. Hu J: miR-31 shuttled by halofuginone-induced exosomes suppresses MFC-7 cell proliferation by modulating the HDAC2/cell cycle signaling axis. *J Cell Physiol*. 2019;234:18970–18984.

8. Li F, Tanaka K, Watanabe S, Tezuka Y, Saiki I. Dipasperoside A, a novel pyridine alkaloid-coupled iridoid glucoside from the roots of *Dipsacus asper. Chem. Pharm. Bull*. 2013;61(12):1318–1322. doi:10.1248/cpb.c13-00546

9. Gong L, Yang S, Liu H, et al. Anti-nociceptive and anti-inflammatory potentials of Akebia saponin D. *European Journal of Pharmacology*. 2019;845:85–90.

10. Chun JM, Lee AY, Nam JY, et al. Effects of Dipsacus asperoides extract on monosodium iodoacetate–induced osteoarthritis in rats based on gene expression profiling. *Front Pharmacol*. 2021;12:615157. doi:10.3389/fphar.2021.615157

11. Wong RW, Rabie ABM, Hägg EUO. The effect of crude extract from Radix Dipsaci on bone in mice. *Phytother Res*. 2007;21(6):596–598. doi:10.1002/ptr.2126

12. Ji D, Wu Y, Zhang B, Zhang C-F, Yang Z-L. Triterpene saponins from the roots of Dipsacus asper and their protective effects against the Aβ25–35 induced cytotoxicity in PC12 cells. *Fitoterapia*. 2012;83(5):843–848. doi:10.1016/j.fitote.2012.03.004

13. Jeong S-I, Zhou B, Bae J-B, et al. Apoptosis-inducing effect of akebia saponin D from the roots of Dipsacus asper Wall in U937 cells. *Arch. Pharmacal Res*. 2008;31(11):1399–1404. doi:10.1007/s12272-001-2123-0

14. Telang NT. Natural products as drug candidates for breast cancer (Review). *Oncol Lett*. 2023;26(2):349. doi:10.3892/ol.2023.13935

15. Chen J, Yao D, Yuan H, et al. Dipsacus asperoides polysaccharide induces apoptosis in osteosarcoma cells by modulating the PI3K/Akt pathway. *Carbohydr Polym*. 2013;95(2):780–784. doi:10.1016/j.carbpol.2013.03.009

16. Unni KK. Osteosarcoma of bone. *J Orthop Sci*. 1998;3(5):287–294. doi:10.1007/s007760050055

17. Longhi A, Ferrari S, Tamburini A, et al. Late effects of chemotherapy and radiotherapy in osteosarcoma and Ewing sarcoma patients: the Italian Sarcoma Group Experience (1983–2006). *Cancer*. 2012;118(20):5050–5059. doi:10.1002/cncr.27493

18. Zhang J, Li S, Li L, et al. Exosome and exosomal microRNA: trafficking, sorting, and function. *Genomics Proteomics Bioinf*. 2015;13(1):17–24. doi:10.1016/j.gpb.2015.02.001

19. Kim J, Li S, Zhang S, Wang J. Plant-derived exosome-like nanoparticles and their therapeutic activities. *Asian J Pharm Sci*. 2022;17(1):53–69. doi:10.1016/j.ajps.2021.05.006

20. Cao M, Diao N, Cai X, et al. Plant exosome nanovesicles (PENs): green delivery platforms. *Mater Horiz*. 2023;10(10):3879–3894. doi:10.1039/D3MH01030A

21. Teng Y, Ren Y, Sayed M, et al. Plant-derived exosomal MicroRNAs shape the gut microbiota. *Cell Host Microbe*. 2018;24(5):637–652 e638. doi:10.1016/j.chom.2018.10.001

22. Ju S, Mu J, Dokland T, et al. Grape exosome-like nanoparticles induce intestinal stem cells and protect mice from DSS-induced colitis. *Mol Ther*. 2013;21:1345–1357.

23. Zhou H, Hu X, Li N, et al. Loganetin and 5-fluorouracil synergistically inhibit the carcinogenesis of gastric cancer cells via down-regulation of the Wnt/beta-catenin pathway. *J Cell Mol Med*. 2020;24(23):13715–13726. doi:10.1111/jcmm.15932

24. Xiang J, Huang JC, Xu C, et al. 甘草水提物中miＲNA 对人免疫细胞基因表达的影响 [Effect of miRNA from Glycyrrhiza uralensis decoction on gene expression of human immune cells]. *Zhongguo Zhong Yao Za Zhi*. 2017;42(9):1752–1756. Chinese. doi:10.19540/j.cnki.cjcmm.2017.0068

25. Cuadrado A, Nebreda AR. Mechanisms and functions of p38 MAPK signalling. *Biochem J*. 2010;429(3):403–417. doi:10.1042/BJ20100323

26. Sun Y, Liu WZ, Liu T, Feng X, Yang N, Zhou HF. Signaling pathway of MAPK/ERK in cell proliferation, differentiation, migration, senescence and apoptosis. *J Recept Signal Transduction Res*. 2015;35(6):600–604. doi:10.3109/10799893.2015.1030412